HHS Public Access

Author manuscript

Hepatology. Author manuscript; available in PMC 2017 October 01.

Published in final edited form as:

Hepatology. 2016 October ; 64(4): 1072–1085. doi:10.1002/hep.28712.

FXR Activation Increases Reverse Cholesterol Transport by Modulating Bile Acid Composition and Cholesterol Absorption

Yang Xu[1], **Fei Li**[2], **Munaf Zalzala**[1,3], **Jiesi Xu**[1], **Frank J Gonzalez**[2], **Luciano Adorini**[4], **Yoon-Kwang Lee**[1], **Liya Yin**[1], and **Yanqiao Zhang**[1]

[1]Department of Integrative Medical Sciences, Northeast Ohio Medical University, Rootstown, OH 44272, USA

[2]Laboratory of Metabolism, Center for Cancer Research, National Cancer Institute, NIH, Bethesda, MD 20892, USA

[3]Department of pharmacology and Toxicology, College of Pharmacy, University of Baghdad, Baghdad, Iraq

[4]Intercept Pharmaceuticals, New York, NY 10014, USA

Abstract

Activation of farnesoid X receptor (FXR) markedly attenuates the development of atherosclerosis in animal models. However, the underlying mechanism is not well elucidated. Here we show that the FXR agonist obeticholic acid (OCA) increases fecal cholesterol excretion and macrophage reverse cholesterol transport (RCT) dependent on activation of hepatic FXR. OCA does not increase biliary cholesterol secretion but inhibits intestinal cholesterol absorption. OCA markedly inhibits hepatic cholesterol 7α-hydroxylase (*Cyp7a1*) and sterol 12α-hydroxylase (*Cyp8b1*) partly through inducing small heterodimer partner (*Shp*), leading to reduced bile acid pool size and altered bile acid composition, with the α/β-muricholic acid proportion in the bile increased by 2.6 fold and taurocholic acid (TCA) level reduced by 71%. Over-expression of *Cyp8b1* or concurrent over-expression of *Cyp7a1* and *Cyp8b1* normalizes TCA level, bile acid composition and intestinal cholesterol absorption.

Conclusions—Our data indicate that activation of FXR inhibits intestinal cholesterol absorption via modulation of bile acid pool size and composition, thus leading to increased RCT. Targeting hepatic FXR and/or bile acids may be useful for boosting RCT and preventing the development of atherosclerosis.

Corresponding authors: Yanqiao Zhang, MD, Department of Integrative Medical Sciences, Northeast Ohio Medical University, Phone: (330) 325-6693, Fax: (330) 325-5978, yzhang@neomed.edu. Liya Yin, MD, PhD, Department of Integrative Medical Sciences, Northeast Ohio Medical University, Phone: (330) 325-6521, lyin@neomed.edu.

Author contributions

Y.X., F.L. M.Z., J.X., L.Y. and Y.Z. performed studies. Y.X. L.Y. and Y.Z. designed and analyzed the data. F.J.G. provided $Fxr^{fl/fl}$ mice and helped analyze bile acid composition. L.A. provided the OCA compound. Y.L. provided $Shp^{-/-}$ mice. L.Y. and Y.Z. wrote the manuscript. All authors reviewed the manuscript.

Competing Financial Interests

The authors declare no competing financial interests.

Keywords

FXR; reverse cholesterol transport; bile acid; OCA; cholesterol absorption

Introduction

The farnesoid X receptor (FXR) is a nuclear hormone receptor that regulates multiple biological processes. FXR plays an important role in regulating bile acid, lipid and glucose metabolism, inflammation and energy homeostasis (1–3). Activation of FXR improves insulin sensitivity, lowers blood and hepatic triglycerides and blood cholesterol, and inhibits hepatic inflammatory response (4–7). In addition, activation of FXR increases macrophage reverse cholesterol transport (RCT) (8), a process that delivers cholesterol from peripheral macrophages to the liver for secretion to the bile and feces. Macrophage RCT is known to be athero-protective (9, 10). Consistent with the role of FXR in RCT and triglyceride (TG) metabolism, activation of FXR is shown to protect against the development of atherosclerosis (11, 12) and non-alcoholic fatty liver disease (NAFLD) (13). Given all these beneficial effects, FXR has been considered an attractive therapeutic target for treatment of metabolic disorders (14, 15).

FXR is highly expressed in the liver, intestine, kidney and adrenal gland, but is undetectable in macrophages (16). Thus, activation of FXR affects the development of atherosclerosis likely through modulating plasma lipid levels. We have previously shown that activation of FXR lowers plasma high density lipoprotein (HDL) level by inducing scavenger receptor group B type 1 (SR-BI) (8). Over-expression of SR-BI is shown to lower plasma HDL-C level, promote RCT and protect against atherosclerosis (17, 18). Consequently, activation of FXR also increases macrophage RCT (8). So far, the mechanism underlying FXR-induced of RCT is not well elucidated.

Cholesterol absorption is an important component of RCT. About ~ 50% dietary or biliary cholesterol is absorbed in the intestine. Therefore, inhibition of intestinal cholesterol absorption promotes RCT (19–21). As amphipathic molecules, bile acids are important regulators of cholesterol absorption. Among all the bile acids, cholic acid (CA) has the most capability to promote cholesterol absorption whereas muricholic acids (MCA) are the strongest inhibitors of cholesterol absorption (22). FXR plays an essential role in all aspects of bile acid metabolism, including bile acid synthesis, conjugation, secretion, absorption and uptake by hepatocytes (23). Classic bile acid synthesis is controlled mainly by two rate-limiting enzymes cholesterol 7α-hydroxylase (CYP7A1) and sterol 12α-hydroxylase (CYP8B1), which are inhibited by FXR. CYP8B1 determines the production rate of CA.

In this study, we used global and tissue-specific *Fxr*$^{-/-}$ mice to investigate how FXR regulates RCT. Our data show that the FXR agonist obeticholic acid (OCA) increases fecal cholesterol excretion and macrophage RCT through activation of hepatic FXR. Such an effect coincides with unchanged biliary cholesterol secretion. Activation of FXR inhibits intestinal cholesterol absorption by altering bile acid pool size and composition and this effect is abolished by over-expression of CYP8B1 or CYP7A1 plus CYP8B1. These data

demonstrate that activation of FXR increases RCT by regulating bile acid synthesis and composition and subsequent inhibition of intestinal cholesterol absorption.

Experimental Procedures

Mice, FXR ligands and adenoviruses

C57BL/6 mice, *Fxr*$^{-/-}$ mice, albumin-Cre mice and vilin-Cre were purchased from the Jackson Laboratories (Bar Harbor, Maine, USA). *Fxr*$^{fl/fl}$ mice (24) and *Shp*$^{-/-}$ mice (25) have been described previously. Liver- or intestine-specific *Fxr*$^{-/-}$ mice were generated by crossing albumin-Cre mice or vilin-Cre mice with *Fxr*$^{fl/fl}$ mice. Where indicated, 10–12 week old mice were gavaged with either vehicle (0.5% carboxymethycellulose, Sigma) or vehicle containing GW4064 (30 mg/kg, twice a day) or OCA (40 mg/kg) for 6–9 days. Adenoviruses expressing rat *Cyp7a1* (Ad-rCyp7a1) (26), mouse *Cyp8b1* (Ad-mCyp8b1) (27), FXRα1-VP16 and FXRα2-VP16 (4) have been described previously. Unless otherwise stated, the mice were euthanized 7 days post injection. In general, all mice were fasted for 5–6 h prior to euthanization. All the animal experiments were approved by the Institutional Animal Care and Use Committee at Northeast Ohio Medical University.

Chemical reagents and antibodies

TRIzol was purchased from Invitrogen (Carlsbad, CA). A reverse-transcription kit was purchased from Applied Biosystems (Foster City, CA). CYP7A1 antibody was a general gift from Dr. David Russel at University of Texas Southwestern Medical Center. CYP8B1 antibody was purchased from Santa Cruz Biotechnology (Santa Cruz, CA). Calnexin and β-actin were purchased from Novus Biologicals (Littleton, CO).

Real-time PCR

RNA was isolated using TRIzol Reagent. mRNA levels were determined by quantitative reverse-transcription polymerase chain reaction (qRT-PCR) on a 7500 real-time PCR machine from Applied Biosystems (Foster City, CA) by using SYBR Green Supermix (Roche, Indianapolis, IN). Results were calculated using *Ct* values and normalized to *36B4* mRNA level.

Western blot assays

Western blot assays were performed using whole liver lysates (4) or nuclear extracts of the liver samples (28, 29) as described previously. The gel band intensity was quantified using the ImageJ software and normalized to β-actin or histone.

Lipid and lipoprotein analysis

Approximately 100 mg liver tissue was homogenized in methanol and lipids were extracted in chloroform/methanol (2:1 v/v) as described (30). Hepatic triglyceride and cholesterol levels were then quantified using Infinity reagents from Thermo Scientific (Waltham, MA). Plasma triglyceride and cholesterol levels were also determined using Infinity reagents. FPLC analysis of lipoprotein profile was performed as described previously (29, 31).

Bile acid level and composition

Bile acids in the liver, intestine and gallbladder were extracted using ethanol. Bile acid levels in the liver, intestine, gallbladder or plasma were measured using a bile acid kit (Diazyme, San Diego, CA). Total bile acids in the liver, intestine and gallbladder were used for calculation of total bile acids/bile acid pool size. Individual bile acids were quantified on a Waters Acquity H-Class UPLC system using a Waters Acquity BEH C18 column (2.1 × 100 mm) coupled to a Waters Xevo G2 QTOFMS, as described (32).

Gallbladder cannulation

Mice were fasted for 4 h followed by anaesthesia. The lower end of the common bile duct was ligated and the gallbladder cannulated below the entrance of the cystic duct using a PE-10 catheter (Becton Dicksinson, Sparks, MD). After successful catheterization and flow of fistula bile, the cystic duct was doubly ligated. Hepatic bile was collected by gravity for the first 1–2 hour.

In vivo reverse cholesterol transport (RCT)

The *in vivo* RCT was performed essentially as described previously (8, 33). Briefly, J774 macrophages (ATCC, Virginia), grown in suspension in DMEM containing 10% FBS and penicillin/streptomycin, were cultured in un-coated cell culture dishes. To load cells with ^{3}H-cholesterol and acetylated LDL (acLDL), J774 cells were incubated in DMEM/10% FBS containing 5 μCi/ml ^{3}H-cholesterol and 25 μg/ml acLDL for 48 h, followed by wash in PBS and equilibration for 4 h in DMEM supplemented with 0.2% BSA and penicillin/streptomycin. Before injection, cells were pelleted and re-suspended in Eagle's minimum essential medium (EMEM, ATCC, VA). All the mice were caged individually with free access to water and food. Mice were injected intraperitoneally with 0.5 ml of J774 cells (typically 5 x10^{6} cells) in EMEM containing 6.5–10x10^{6} counts per minute (cpm). Blood was collected at 24 h and 48 h and plasma ^{3}H-tracers were assayed using a liquid scintillation counter (LSC). Feces were collected continuously from 0 to 48 h. At the end of the experiment, mice were perfused with cold PBS. A portion of the liver was removed for lipid and RNA extraction.

Approximately 100 mg liver was homogenized in methanol and lipids were extracted in chloroform/methanol (2:1 v/v) as described (30). The lipids were collected, dried and re-suspended in toluene and counted in an LSC.

Fecal cholesterol and bile acids

Fecal total sterols, cholesterol and bile acids (BAs) were extracted as described (8, 33). The radioactivity was measured using an LSC. For mice that were not given any radioisotopes, feces were collected consecutively for 48 h. After total sterols, cholesterol and bile acids were extracted, free cholesterol and total bile acids were measured using a free cholesterol kit (Wako USA, Richmond, VA) or total bile acid kit (Diazyme, San Diego, CA).

Intestinal cholesterol absorption

Intestinal cholesterol absorption was performed as described previously (8, 34). Briefly, mice were injected with 2.5 μCi ^{3}H-cholesterol in Intralipid (Sigma) via tail vein injection, followed by immediate gavage with 1 μCi ^{14}C-cholesterol in median-chain triglycerides (MCT oil, Mead Johnson, Evansville, IN). After 72 h, blood and tissue were collected. The percent of the intestinal cholesterol absorption was calculated using the formula: [percent of intragastric dose (^{14}C-cholesterol) per ml plasma] ÷ [percent of intravenous dose (^{3}H-cholesterol) per ml plasma] x 100.

Statistical analysis

Statistical significance was analyzed using unpaired Student *t* test or ANOVA (GraphPad Prism, CA). All values are expressed as mean±SEM. Differences were considered statistically significant at $P<0.05$.

Results

OCA lowers plasma cholesterol and increases fecal cholesterol excretion through activation of hepatic FXR

To investigate how FXR activation increases RCT, we treated *Fxr*$^{-/-}$ mice and their wild-type littermates with either vehicle or the semi-synthetic FXR agonist OCA for 7 days. OCA lowered plasma total cholesterol in wild-type mice but not in *Fxr*$^{-/-}$ mice (Figure 1A). Such a reduction in plasma cholesterol level was due to decreased plasma HDL-C level (data not shown). OCA also increased fecal free cholesterol level (Figure 1B, left panel) but reduced fecal bile acid level (Figure 1B, right panel) in wild-type mice but not in *Fxr*$^{-/-}$ mice. These data demonstrate that OCA lowers plasma cholesterol and increases fecal free cholesterol level via activation of FXR.

FXR is highly expressed in both the liver and intestine. To determine whether OCA regulates cholesterol metabolism via activation of hepatic and/or intestinal FXR, we treated liver-specific *Fxr*$^{-/-}$ (*L-Fxr*$^{-/-}$) mice, intestine-specific *Fxr*$^{-/-}$ (*I-Fxr*$^{-/-}$) mice and their control littermates (*Fxr*$^{fl/fl}$ mice) with either vehicle or OCA for 7 days. OCA lowered plasma cholesterol (Figure 1C) and increased fecal free cholesterol level (Figure 1D, left panel) in the control mice but not in *L-Fxr*$^{-/-}$ mice. In addition, OCA reduced fecal bile acid levels in both genotypes (Figure 1D, right panel).

In contrast to what was observed in *L-Fxr*$^{-/-}$ mice, OCA reduced plasma cholesterol and increased fecal free cholesterol level in both the control mice and *I-Fxr*$^{-/-}$ mice (Figure 1E and 1F, left panel), but reduced fecal bile acid level only in the control mice (Figure 1F, right panel). Collectively, the data of Figure 1 indicate that OCA reduces plasma cholesterol and increases fecal cholesterol level via activation of hepatic FXR whereas the reduction in fecal bile acids is dependent on activation of intestinal FXR.

OCA inhibits CYP7A1 and CYP8B1 expression through activation of hepatic and/or intestinal FXR and partly through SHP

To determine whether OCA functioned properly in animals, we analyzed hepatic gene expression. As expected, OCA induced *Shp* (small heterodimer partner), a well-characterized FXR target gene, and repressed *Cyp7a1* and *Cyp8b1* mRNA levels in wild-type mice but not in $Fxr^{-/-}$ mice (Figure 2A). However, the repression of *Cyp7a1* or *Cyp8b1* was mitigated or abolished in $L\text{-}Fxr^{-/-}$ mice (Figure 2B) or $I\text{-}Fxr^{-/-}$ mice (Figure 2C), suggesting that OCA represses *Cyp7a1* and *Cyp8b1* expression via activation of hepatic and/or intestinal FXR. Previous studies show that activation of FXR induces intestinal expression of FGF15, an enterohepatic hormone, to repress hepatic CYP7A1 and CYP8B1 expression (35, 36). In $I\text{-}Fxr^{-/-}$ mice, OCA treatment completely failed to inhibit *Cyp7a1* and only partially inhibited *Cyp8b1* (Figure 2C), which may explain why OCA treatment reduces fecal bile acid levels dependent on activation of intestinal FXR (Figure 1F).

SHP is known to inhibit bile acid synthesis (25, 37). To determine whether *Shp* is required for FXR to inhibit both *Cyp7a1* and *Cyp8b1*, we gavaged wild-type mice and $Shp^{-/-}$ mice with vehicle or the specific FXR agonist GW4064 for 7 days. The data of Figure 2D show that GW4064 markedly reduced both *Cyp7a1* and *Cyp8b1* expression and such a reduction was greatly attenuated in $Shp^{-/-}$ mice, indicating that activation of FXR represses *Cyp7a1* and *Cyp8b1* expression partly through induction of SHP.

Consistent with the involvement of both hepatic and intestinal FXR in regulating CYP7A1 and CYP8B1 expression, OCA treatment reduced bile acid levels in the liver and gallbladder or intestine dependent on activation of hepatic or intestinal FXR, respectively (Figure 2E). In addition, both hepatic and intestinal FXR were required for OCA to reduce the bile acid pool size (Figure 2E) or plasma bile acid level (Figure S1). OCA did not lower plasma bile acid levels in global $Fxr^{-/-}$ mice (data not shown). Together, the data of Figure 2 demonstrate that suppression of CYP7A1 and CYP8B1 expression and the bile acid pool size involves activation of hepatic and/or intestinal FXR and its downstream target SHP.

Hepatic FXR is required for OCA to increase macrophage RCT

The data of Figure 1 suggest that OCA increases fecal free cholesterol excretion and lowers plasma cholesterol level via activation of hepatic FXR. Analysis of plasma lipoprotein profile by fast protein liquid chromatography (FPLC) indicates that OCA lowers plasma cholesterol levels in the control littermates primarily by reducing HDL-C (Figure 3A). In addition, there was an increase in LDL-C in $L\text{-}Fxr^{-/-}$ mice (Figure 3A). Since HDL plays an important role in RCT, we determined the role of hepatic FXR in macrophage RCT.

Forty-eight hours after injection of J774 macrophages loaded with [^{3}H]cholesterol and acetylated LDL, blood radioactivity was significantly reduced (Figure 3B) whereas fecal [^{3}H]total sterols (Figure 3C) as well as [^{3}H]free cholesterol level (Figure 3D) were significantly increased in OCA-treated control littermates but these changes were not observed in $L\text{-}Fxr^{-/-}$ mice. There was not much change in fecal [^{3}H]bile acid level (Figure 3E) or hepatic radioactivity (data not shown) in both genotypes. The unchanged fecal [^{3}H]bile acid level is likely a net result of increased transport of [^{3}H]cholesterol from

macrophages to the liver via SR-BI and an inhibition of bile acid biosynthesis. Lastly, OCA treatment significantly reduced hepatic *Cyp7a1* mRNA level (Figure 3F) but induced *SR-BI* mRNA and protein levels (Figure S2), indicating that OCA functioned properly *in vivo*. Thus, the data of Figure 3 demonstrate that hepatic FXR activation is required for OCA to increase macrophage RCT.

Activation of FXR does not increase biliary cholesterol secretion

Biliary cholesterol secretion plays an important role in RCT. Since hepatic FXR activation is required for OCA-induced macrophage RCT, we investigated whether activation of FXR increased biliary cholesterol secretion. FXR has four isoforms. Previous data suggest that FXRα1 and FXRα2 may have similar functions as FXRα3 and FXRα4, respectively (16). Therefore, we over-expressed FXRα1-VP16 or FXRα2-VP16 in the liver to constitutively activate FXRα1 or FXRα2. As expected, activation of FXRα1 or FXRα2 markedly inhibited bile acid secretion (Figure 4A, left panel). However, activation of FXRα2 but not FXRα1 inhibited bile flow (Figure 4A, middle panel) and reduced biliary cholesterol secretion (Figure 4A, right panel). Consistent with these observations, activation of FXRα1 or FXRα2 markedly inhibited *Cyp7a1* and *Cyp8b1* expression (Figure 4B). Interestingly, activation of FXRα1 induced bile salt export protein (*Bsep*) by ~ 9 fold whereas activation of FXRα2 induced *Bsep* only by ~ 2.3 fold (Figure 4B). In addition, activation of FXRα1 but not FXRα2 induced multidrug resistance protein 2 (*Mdr2*) and ATP-binding cassette subgroup G member 5 (*Abcg5*) expression (Figure 4B). Neither FXRα1 nor FXRα2 activation had an effect on *Abcg8* expression (Figure 4B).

We next investigated whether the specific FXR agonist GW4064 had similar effects as constitutively activated FXR (FXR-VP16) in the liver. Treatment of mice with GW4064 had no effect on bile flow (Figure 4C) or biliary cholesterol secretion (Figure 4D). In a macrophage RCT study, we did not see any change in biliary [^{3}H] radioactivity following GW4064 treatment (Figure 4E). In addition, GW4064 treatment significantly induced *Shp* and *Bsep* but inhibited *Cyp7a1* and *Cyp8b1* (Figure 4F), suggesting that GW4064 functioned properly *in vivo*.

Studies with another specific FXR agonist OCA produced similar results. OCA treatment reduced bile acid secretion in wild-type but not in $Fxr^{-/-}$ mice (Figure S3A), and had no effect on bile flow (Figure S3B) or biliary cholesterol secretion (Figure S3C) in wild-type or $Fxr^{-/-}$ mice. Further studies involving liver- or intestine-specific $Fxr^{-/-}$ mice show that OCA inhibited biliary bile acid secretion dependent on activation of both hepatic and intestinal FXR (Figure S3D). OCA treatment had no effect on bile flow in $Fxr^{fl/fl}$ mice, $L\text{-}Fxr^{-/-}$ mice or $I\text{-}Fxr^{-/-}$ mice (Figure S3E). Together, the data of Figure 4 and Figure S3 demonstrate that activation of FXR does not increase biliary cholesterol secretion and inhibits bile acid secretion via activation of both hepatic and intestinal FXR.

Activation of FXR reduces intestinal cholesterol absorption primarily through inhibition of hepatic CYP8B1

Intestinal cholesterol absorption plays an important role in cholesterol homeostasis and is an important component of RCT. Bile acids play a critical role in regulating cholesterol

absorption with CA being the most efficient bile acid in promoting cholesterol absorption. In the classic pathway of bile acid biosynthesis, CYP7A1 catalyzes the rate-limiting step whereas CYP8B1 determines the rate of CA biosynthesis (Figure 5A). As shown in Figure 5B, OCA treatment significantly inhibited cholesterol absorption. This inhibition was due to activation of hepatic FXR as OCA was able to inhibit intestinal cholesterol absorption in *I-Fxr*$^{-/-}$ mice but not in *L-Fxr*$^{-/-}$ mice (Figure S4). Since FXR activation markedly inhibited both *Cyp7a1* and *Cyp8b1* expression, we asked whether recapitulation of hepatic *Cyp7a1* and/or *Cyp8b1* levels would prevent FXR-induced inhibition of cholesterol absorption. Over-expression of *Cyp7a1* (from rat cDNA) and/or *Cyp8b1* (from mouse cDNA) had no effect on intestinal cholesterol absorption in vehicle-treated mice (Figure S5A–D). Concurrent expression of *Cyp7a1* and *Cyp8b1* or over-expression of *Cyp8b1* alone, but not *Cyp7a1* alone, recovered intestinal cholesterol absorption to the normal level in OCA-treated mice (Figure 5B). OCA markedly inhibited endogenous *Cyp7a1* mRNA level (Figure 5C), and re-expression of *Cyp7a1* was able to recapitulate hepatic CYP7A1 protein level to the normal level (Figure 5D). The data of Figure 5D and Figure 5E show that OCA markedly inhibited hepatic levels of *Cyp8b1* mRNA and protein, which were reversed by *Cyp8b1* over-expression. Taken together, the data of Figure 5 and Figure S5 demonstrate that activation of FXR inhibits intestinal cholesterol absorption primarily through inhibition of hepatic CYP8B1 expression.

Over-expression of CYP8B1 or CYP7A1 plus CYP8B1 prevents FXR-induced increase in muricholic acid level and decrease in taurocholic acid level

To determine how over-expression of CYP7A1 and CYP8B1 prevents FXR-induced inhibition of intestinal cholesterol absorption, we analyzed bile acid pool size and bile acid composition. As expected, over-expression of *Cyp7a1* and/or *Cyp8b1* increased bile acid levels in the intestine, liver and/or gallbladder as well as total bile acid levels in vehicle-treated mice (Figure S6A–D). Activation of FXR by OCA significantly reduced (Figure 6A and 6B) or tended to (Figure 6C) reduce bile acid level in the intestine (Figure 6A), liver (Figure 6B) and gallbladder (Figure 6C). As a result, OCA significantly reduced the bile acid pool size by 76% (Figure 6D). Over-expression of *Cyp7a1* alone in OCA-treated mice partly or completely recovered bile acid levels in the intestine (Figure 6A), liver (Figure 6B) and gallbladder (Figure 6C), and partly recovered total bile acid levels (Figure 6D). In contrast, concurrent expression of both *Cyp7a1* and *Cyp8b1* or *Cyp8b1* over-expression alone completely recovered or increased bile acid levels in the intestine, liver and gall bladder as well as total bile acid levels in OCA-treated mice (Figure 6A–6D). Interestingly, although over-expression of *Cyp7a1* or *Cyp8b1* increased intestinal bile acid levels to a similar extent in OCA-treated mice (Figure 6A), *Cyp8b1*, but not *Cyp7a1*, over-expression was able to normalize cholesterol absorption (Figure 5B).

Analysis of individual bile acid levels in the bile indicated that OCA treatment reduced by 71% the levels of taurocholic acid (TCA), the most abundant bile acid, whereas concurrent expression of both *Cyp7a1* and *Cyp8b1* or *Cyp8b1* over-expression alone recapitulated TCA level to the normal level (Figure 6E). OCA treatment also significantly reduced deoxycholic acid (DCA) and taurodeoxycholic acid (TDCA) levels, which could not be recovered to the normal levels by *Cyp8b1* or *Cyp7a1* plus *Cyp8b1* over-expression (Figure 6E). In contrast,

OCA treatment had no much effect on the levels of CA, α/β-muricholic acid (α/β-MCA), taurochenodeoxycholic acid (TCDCA) or tauroursodeoxycholic acid (TUDCA) (Figure 6E).

Further analysis of bile acid composition in the bile indicated that OCA treatment increased the relative levels of α/β-MCA from 11.3% to 29.4% and this increase was blunted by over-expression of *Cyp8b1* alone or *Cyp7a1* plus *Cyp8b1* but not by over-expression of *Cyp7a1* alone (Figure 6F). Since MCAs are the most hydrophilic bile acids and the most potent inhibitors of cholesterol absorption whereas cholic acids (CA and TCA) are the most potent promoters of cholesterol absorption among all the bile acids (22), the data of Figure 6 suggest that the changes in MCA and CA levels are responsible for the reduced cholesterol absorption following OCA treatment.

Discussion

Atherosclerosis is the leading cause of coronary heart disease. Activation of FXR has been shown to increase RCT (8) and protects against the development of atherosclerosis in *Ldlr*$^{-/-}$ or *Apoe*$^{-/-}$ mice (11, 12). In addition, activation of FXR also lowers TG levels and inhibits inflammation in the liver, thus preventing the development of NAFLD (13). Finally, activation of FXR improves insulin sensitivity in diabetic mice or humans (4–6). These observations have suggested that FXR is a therapeutic target for treatment of common metabolic disorders, including NAFLD, atherosclerosis and insulin resistance. However, the mechanism underlying the regulation of RCT by FXR is not well elucidated. By using tissue-specific *Fxr*$^{-/-}$ mice, herein we show that activation of FXR increases RCT by suppression of hepatic bile acid synthesis, alternation of bile acid composition and subsequent inhibition of intestinal cholesterol absorption, a novel pathway that is independent of the canonical biliary secretion route.

Our previous data show that activation of FXR increases macrophage RCT through a pathway that requires SR-BI (8). Since FXR activation induces SR-BI expression in the liver (8), one may speculate that FXR activation likely increases biliary cholesterol secretion. By using tissue-specific *Fxr*$^{-/-}$ mice, we show that the synthetic FXR agonist OCA increases macrophage RCT through activation of hepatic FXR. However, neither constitutive activation of FXR in the liver nor GW4064 or OCA treatment increases biliary cholesterol secretion. This latter observation supports the recent findings that intestine is capable of modulating RCT directly (38). In addition, our data show that FXR activation significantly inhibits biliary bile acid secretion. Given that FXR activation is known to increase phospholipid secretion, our observations raise that possibility that FXR activation may increase the formation of cholesterol gallstone.

The role of FXR in controlling bile acid homeostasis has been well established. Our data indicate that OCA represses both CYP7A1 and CYP8B1 expression via activation of hepatic and intestinal FXR and partly through inducing SHP. Over-expression of CYP8B1 or CYP7A1 plus CYP8B1 is sufficient to prevent OCA-induced inhibition of intestinal cholesterol absorption, demonstrating that activation of FXR inhibits intestinal cholesterol absorption via modulating bile acid metabolism. Gardes *et al* have reported that synthetic FXR agonists, including OCA (also called 6E-CDCA), GW4064, R05186026 and X-Ceptor

compound, all inhibit intestinal cholesterol absorption, reduce bile acid pool size, and decrease fecal bile acid excretion in *Ldlr*$^{-/-}$ mice that are fed a Western diet (39), a known atherogentic mouse model. Thus, the studies by us and Gardes *et al* indicate that activation of FXR inhibits intestinal cholesterol absorption in both wild-type (normal) mice and atherogenic mice by regulating bile acid metabolism. Activation of intestinal FXR has been shown to inhibit hepatic CYP7A1 expression via FGF15/19 (35). However, recapitulation of hepatic CYP7A1 expression has no effect on FXR-induced inhibition of intestinal cholesterol absorption, supporting the finding that hepatic FXR activation is responsible for induction of RCT.

Hydrophobic bile acids, such as CA and DCA, promote cholesterol absorption whereas hydrophilic bile acids, such as MCAs, are potent inhibitors of cholesterol absorption (22). In hamsters, TCA is identified as a potential plasma biomarker of early atheromatous plaque formation (40). Our data show that OCA reduces hydrophobic bile acid (CA and DCA) level by ~ 71% and increases the relative level of α/β-MCAs by 2.6 fold. Over-expression of CYP8B1 alone or CYP7A1 plus CYP8B1, but not CYP7A1 alone, reverses OCA-induced changes in bile acid level (TCA), bile acid composition (TCA and α/β-MCAs) and cholesterol absorption. Interestingly, over-expression of CYP8B1 alone or CYP7A1 plus CYP8B1 does not restore DCA/TDCA levels, suggesting that OCA inhibits cholesterol absorption through inhibition of CA/TCA synthesis and induction of α/β-MCA levels. Over-expression of CYP7A1 normalizes bile acid pool size by 65% but does not affect cholesterol absorption, suggesting that the change in bile acid pool size *per se* may not contribute to the reduced cholesterol absorption. Since intestinal cholesterol absorption is an important component of RCT, our data suggest that activation of FXR increases RCT by altering bile acid synthesis and composition and subsequently inhibiting intestinal cholesterol absorption.

Our current findings are consistent with previous observations that inhibition of bile acid synthesis increases RCT. *Cyp7a1*$^{-/-}$ mice (41, 42) or *Cyp8b1*$^{-/-}$ mice (43) have reduced intestinal cholesterol absorption and increased fecal sterol secretion. Loss of *Cyp8b1* in *Apoe*$^{-/-}$ mice is shown to inhibit the development of atherosclerosis (44). Therefore, targeting bile acid synthesis may be a useful strategy for prevention of atherogenesis.

Accumulating data have indicated that FXR is an attractive target for treatment of diverse metabolic disorders, including atherosclerosis. The data presented here provide important insights into the mechanism underlying FXR-medicated inhibition of atherosclerosis. In addition, our studies suggest that FXR and bile acids may be targeted for enhancing RCT and thus for preventing the development of atherosclerosis.

Supplementary Material

Refer to Web version on PubMed Central for supplementary material.

Acknowledgments

Financial support: This work was supported by NIH grants R01HL103227, R01DK095895 and R01DK102619 to Y.Z.

References

1. Lefebvre P, Cariou B, Lien F, Kuipers F, Staels B. Role of bile acids and bile acid receptors in metabolic regulation. Physiol Rev. 2009; 89:147–191. [PubMed: 19126757]
2. Zhang Y. Farnesoid X receptor: acting through bile acids to treat metabolic disorders. Drugs of the Future. 2010; 35:635–641. [PubMed: 24465082]
3. Fang S, Suh JM, Reilly SM, Yu E, Osborn O, Lackey D, Yoshihara E, et al. Intestinal FXR agonism promotes adipose tissue browning and reduces obesity and insulin resistance. Nat Med. 2015; 21:159–165. [PubMed: 25559344]
4. Zhang Y, Lee FY, Barrera G, Lee H, Vales C, Gonzalez FJ, Willson TM, et al. Activation of the nuclear receptor FXR improves hyperglycemia and hyperlipidemia in diabetic mice. Proc Natl Acad Sci U S A. 2006; 103:1006–1011. [PubMed: 16410358]
5. Mudaliar S, Henry RR, Sanyal AJ, Morrow L, Marschall HU, Kipnes M, Adorini L, et al. Efficacy and safety of the farnesoid X receptor agonist obeticholic acid in patients with type 2 diabetes and nonalcoholic fatty liver disease. Gastroenterology. 2013; 145:574–582. e571. [PubMed: 23727264]
6. Ma K, Saha PK, Chan L, Moore DD. Farnesoid X receptor is essential for normal glucose homeostasis. J Clin Invest. 2006; 116:1102–1109. [PubMed: 16557297]
7. Li Y, Jadhav K, Zhang Y. Bile acid receptors in non-alcoholic fatty liver disease. Biochem Pharmacol. 2013; 86:1517–1524. [PubMed: 23988487]
8. Zhang Y, Yin L, Anderson J, Ma H, Gonzalez FJ, Willson TM, Edwards PA. Identification of novel pathways that control farnesoid X receptor-mediated hypocholesterolemia. J Biol Chem. 2010; 285:3035–3043. [PubMed: 19996107]
9. Cuchel M, Rader DJ. Macrophage reverse cholesterol transport: key to the regression of atherosclerosis? Circulation. 2006; 113:2548–2555. [PubMed: 16735689]
10. Rosenson RS, Brewer HB Jr, Davidson WS, Fayad ZA, Fuster V, Goldstein J, Hellerstein M, et al. Cholesterol efflux and atheroprotection: advancing the concept of reverse cholesterol transport. Circulation. 2012; 125:1905–1919. [PubMed: 22508840]
11. Hartman HB, Gardell SJ, Petucci CJ, Wang S, Krueger JA, Evans MJ. Activation of farnesoid X receptor prevents atherosclerotic lesion formation in LDLR−/− and apoE−/− mice. J Lipid Res. 2009; 50:1090–1100. [PubMed: 19174369]
12. Flatt B, Martin R, Wang TL, Mahaney P, Murphy B, Gu XH, Foster P, et al. Discovery of XL335 (WAY-362450), a highly potent, selective, and orally active agonist of the farnesoid X receptor (FXR). J Med Chem. 2009; 52:904–907. [PubMed: 19159286]
13. Li Y, Jadhav K, Zhang Y. Bile acid receptors in non-alcoholic fatty liver disease. Biochem Pharmacol. 86:1517–1524. [PubMed: 23988487]
14. Zhang Y, Edwards PA. FXR signaling in metabolic disease. FEBS Lett. 2008; 582:10–18. [PubMed: 18023284]
15. Porez G, Prawitt J, Gross B, Staels B. Bile acid receptors as targets for the treatment of dyslipidemia and cardiovascular disease. J Lipid Res. 2012; 53:1723–1737. [PubMed: 22550135]
16. Zhang Y, Kast-Woelbern HR, Edwards PA. Natural structural variants of the nuclear receptor farnesoid X receptor affect transcriptional activation. J Biol Chem. 2003; 278:104–110. [PubMed: 12393883]
17. Kinoshita M, Fujita M, Usui S, Maeda Y, Kudo M, Hirota D, Suda T, et al. Scavenger receptor type BI potentiates reverse cholesterol transport system by removing cholesterol ester from HDL. Atherosclerosis. 2004; 173:197–202. [PubMed: 15064092]
18. van der Velde AE, Groen AK. Shifting gears: liver SR-BI drives reverse cholesterol transport in macrophages. J Clin Invest. 2005; 115:2699–2701. [PubMed: 16200207]
19. Wang J, Mitsche MA, Lutjohann D, Cohen JC, Xie XS, Hobbs HH. Relative roles of ABCG5/ABCG8 in liver and intestine. J Lipid Res. 2015; 56:319–330. [PubMed: 25378657]
20. Huang Y, Wang J, Quan G, Wang X, Yang L, Zhong L. Lactobacillus acidophilus ATCC 4356 prevents atherosclerosis via inhibition of intestinal cholesterol absorption in apolipoprotein E-knockout mice. Appl Environ Microbiol. 2014; 80:7496–7504. [PubMed: 25261526]

21. Davidson MH, Voogt J, Luchoomun J, Decaris J, Killion S, Boban D, Glass A, et al. Inhibition of intestinal cholesterol absorption with ezetimibe increases components of reverse cholesterol transport in humans. Atherosclerosis. 2013; 230:322–329. [PubMed: 24075764]
22. Wang DQ, Tazuma S, Cohen DE, Carey MC. Feeding natural hydrophilic bile acids inhibits intestinal cholesterol absorption: studies in the gallstone-susceptible mouse. Am J Physiol Gastrointest Liver Physiol. 2003; 285:G494–502. [PubMed: 12748061]
23. Lee FY, Lee H, Hubbert ML, Edwards PA, Zhang Y. FXR, a multipurpose nuclear receptor. Trends Biochem Sci. 2006; 31:572–580. [PubMed: 16908160]
24. Sinal CJ, Tohkin M, Miyata M, Ward JM, Lambert G, Gonzalez FJ. Targeted Disruption of the Nuclear Receptor FXR/BAR Impairs Bile Acid and Lipid Homeostasis. Cell. 2000; 102:731–744. [PubMed: 11030617]
25. Wang L, Lee YK, Bundman D, Han Y, Thevananther S, Kim CS, Chua SS, et al. Redundant pathways for negative feedback regulation of bile acid production. Dev Cell. 2002; 2:721–731. [PubMed: 12062085]
26. Pandak WM, Schwarz C, Hylemon PB, Mallonee D, Valerie K, Heuman DM, Fisher RA, et al. Effects of CYP7A1 overexpression on cholesterol and bile acid homeostasis. Am J Physiol Gastrointest Liver Physiol. 2001; 281:G878–889. [PubMed: 11557507]
27. Pandak WM, Bohdan P, Franklund C, Mallonee DH, Eggertsen G, Bjorkhem I, Gil G, et al. Expression of sterol 12alpha-hydroxylase alters bile acid pool composition in primary rat hepatocytes and in vivo. Gastroenterology. 2001; 120:1801–1809. [PubMed: 11375960]
28. Zhang Y, Yin L, Hillgartner FB. SREBP-1 integrates the actions of thyroid hormone, insulin, cAMP, and medium-chain fatty acids on ACCalpha transcription in hepatocytes. J Lipid Res. 2003; 44:356–368. [PubMed: 12576518]
29. Xu J, Li Y, Chen W, Xu Y, Yin L, Ge X, Jadhav K, et al. Hepatic carboxylesterase 1 is essential for both normal and farnesoid X-receptor-controlled lipid homeostasis. Hepatology. 2013 in press.
30. Bligh EG, Dyer WJ. A rapid method of total lipid extraction and purification. Can J Biochem Physiol. 1959; 37:911–917. [PubMed: 13671378]
31. Xu Y, Zalzala M, Xu J, Li Y, Yin L, Zhang Y. A metabolic stress-inducible miR-34a-HNF4alpha pathway regulates lipid and lipoprotein metabolism. Nat Commun. 2015; 6:7466. [PubMed: 26100857]
32. Jiang C, Xie C, Li F, Zhang L, Nichols RG, Krausz KW, Cai J, et al. Intestinal farnesoid X receptor signaling promotes nonalcoholic fatty liver disease. J Clin Invest. 2015; 125:386–402. [PubMed: 25500885]
33. Naik SU, Wang X, Da Silva JS, Jaye M, Macphee CH, Reilly MP, Billheimer JT, et al. Pharmacological activation of liver X receptors promotes reverse cholesterol transport in vivo. Circulation. 2006; 113:90–97. [PubMed: 16365197]
34. Turley SD, Herndon MW, Dietschy JM. Reevaluation and application of the dual-isotope plasma ratio method for the measurement of intestinal cholesterol absorption in the hamster. J Lipid Res. 1994; 35:328–339. [PubMed: 8169536]
35. Inagaki T, Choi M, Moschetta A, Peng L, Cummins CL, McDonald JG, Luo G, et al. Fibroblast growth factor 15 functions as an enterohepatic signal to regulate bile acid homeostasis. Cell Metab. 2005; 2:217–225. [PubMed: 16213224]
36. Kong B, Wang L, Chiang JY, Zhang Y, Klaassen CD, Guo GL. Mechanism of tissue-specific farnesoid X receptor in suppressing the expression of genes in bile-acid synthesis in mice. Hepatology. 2012; 56:1034–1043. [PubMed: 22467244]
37. Kerr TA, Saeki S, Schneider M, Schaefer K, Berdy S, Redder T, Shan B, et al. Loss of nuclear receptor SHP impairs but does not eliminate negative feedback regulation of bile acid synthesis. Dev Cell. 2002; 2:713–720. [PubMed: 12062084]
38. Brufau G, Groen AK, Kuipers F. Reverse cholesterol transport revisited: contribution of biliary versus intestinal cholesterol excretion. Arterioscler Thromb Vasc Biol. 2011; 31:1726–1733. [PubMed: 21571685]
39. Gardes C, Chaput E, Staempfli A, Blum D, Richter H, Benson GM. Differential regulation of bile acid and cholesterol metabolism by the farnesoid X receptor in Ldlr −/− mice versus hamsters. J Lipid Res. 2013; 54:1283–1299. [PubMed: 23431047]

40. Jove M, Ayala V, Ramirez-Nunez O, Serrano JC, Cassanye A, Arola L, Caimari A, et al. Lipidomic and metabolomic analyses reveal potential plasma biomarkers of early atheromatous plaque formation in hamsters. Cardiovasc Res. 2013; 97:642–652. [PubMed: 23241314]

41. Schwarz M, Russell DW, Dietschy JM, Turley SD. Alternate pathways of bile acid synthesis in the cholesterol 7alpha-hydroxylase knockout mouse are not upregulated by either cholesterol or cholestyramine feeding. J Lipid Res. 2001; 42:1594–1603. [PubMed: 11590215]

42. Erickson SK, Lear SR, Deane S, Dubrac S, Huling SL, Nguyen L, Bollineni JS, et al. Hypercholesterolemia and changes in lipid and bile acid metabolism in male and female cyp7A1-deficient mice. J Lipid Res. 2003; 44:1001–1009. [PubMed: 12588950]

43. Li-Hawkins J, Gafvels M, Olin M, Lund EG, Andersson U, Schuster G, Bjorkhem I, et al. Cholic acid mediates negative feedback regulation of bile acid synthesis in mice. J Clin Invest. 2002; 110:1191–1200. [PubMed: 12393855]

44. Slatis K, Gafvels M, Kannisto K, Ovchinnikova O, Paulsson-Berne G, Parini P, Jiang ZY, et al. Abolished synthesis of cholic acid reduces atherosclerotic development in apolipoprotein E knockout mice. J Lipid Res. 2010; 51:3289–3298. [PubMed: 20675645]

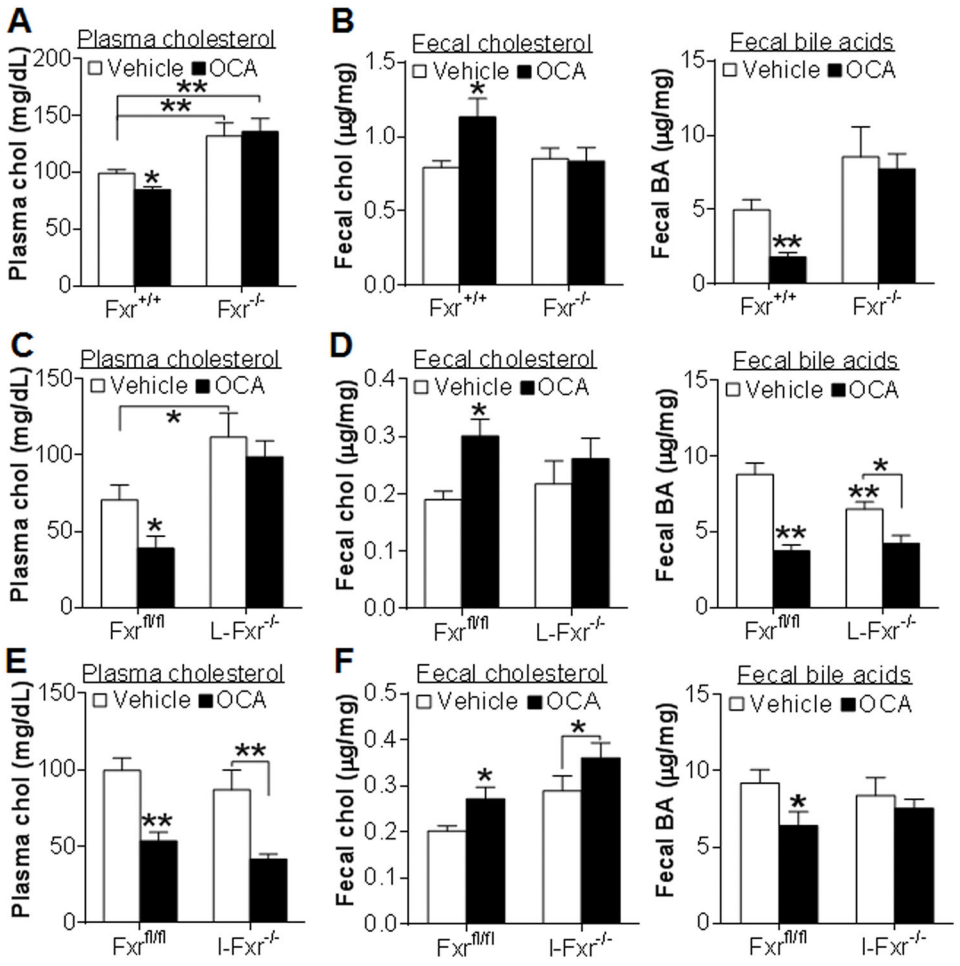

Figure 1. OCA lowers plasma cholesterol and increases fecal cholesterol excretion by activation of hepatic FXR

(**A**, **B**) *Fxr*$^{+/+}$ and *Fxr*$^{-/-}$ mice were treated with either vehicle or OCA for 7 days (n=7–8). Plasma cholesterol (**A**), fecal free cholesterol (**B**, left panel) and fecal bile acid (**B**, right panel) levels were determined. (**C, D**) *Fxr*$^{fl/fl}$ and *L-Fxr*$^{-/-}$ mice were treated with either vehicle or OCA for 7 days (n=8). Plasma cholesterol (**C**), fecal free cholesterol (**D**, left panel) and fecal bile acid (**D**, right panel) levels were determined. (**E, F**) *Fxr*$^{fl/fl}$ and *I-Fxr*$^{-/-}$ mice were treated with either vehicle or OCA for 7 days (n=8). Plasma cholesterol (**E**), fecal free cholesterol (**F**, right panel) and fecal bile acid (**F**, right panel) levels were determined. * $p<0.05$, ** $p<0.01$. Unless otherwise indicated, the difference is shown when compared to vehicle-treated control mice.

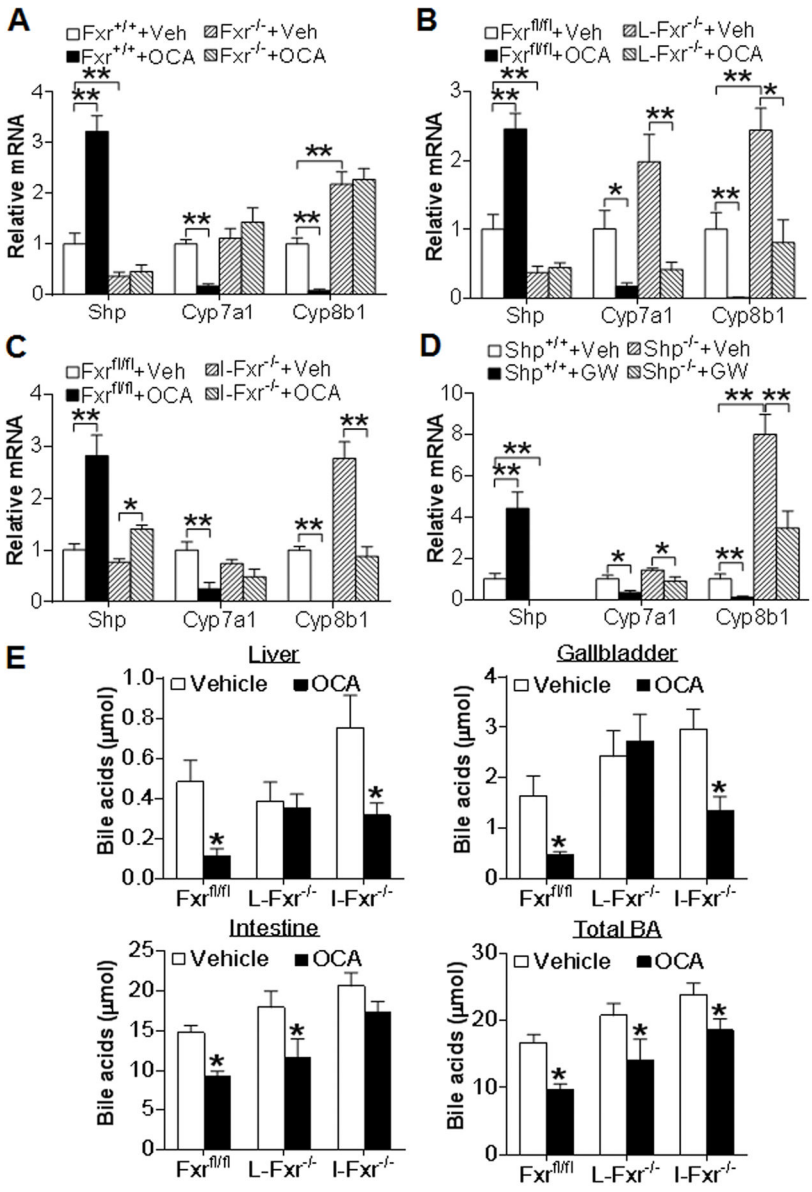

Figure 2. OCA inhibits CYP7A1 and CYP8B1 expression through activation of hepatic and/or intestinal FXR and partly through SHP

(A–C) The liver samples were collected from mice described in the legend of Figure 1. Hepatic mRNA levels in the *Fxr*$^{+/+}$ or *Fxr*$^{-/-}$ mice (**A**), *Fxr*$^{fl/fl}$ or *L-Fxr*$^{-/-}$ mice (**B**) and *Fxr*$^{fl/fl}$ or *I-Fxr*$^{-/-}$ mice (**C**) were determined (n=8). (**D**) *Shp*$^{+/+}$ and *Shp*$^{-/-}$ mice were gavaged with either vehicle or GW4064 for 7 days (n=6). Hepatic mRNA levels were determined. (**E**) *Fxr*$^{fl/fl}$ mice, *L-Fxr*$^{-/-}$ mice and *I-Fxr*$^{-/-}$ mice were gavaged with either vehicle or OCA for 7 days (n=6). Bile acid levels in the liver, gallbladder and intestine as well as total bile acid levels were determined. * p<0.05, ** p<0.01. In (**E**), the difference was compared between the OCA-treated group and the vehicle-treated group of the same genotype.

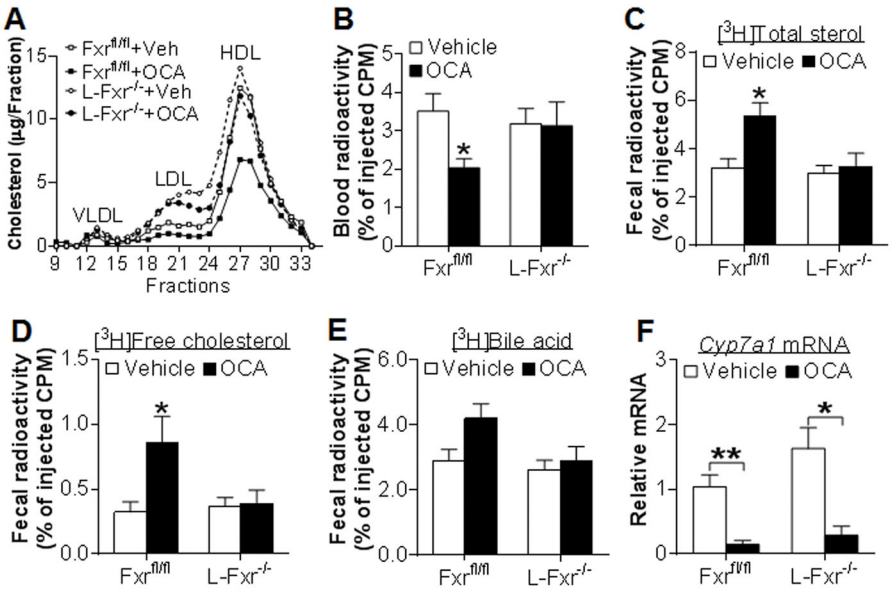

Figure 3. OCA increases macrophage reverse cholesterol transport by activation of hepatic FXR

(**A**) FPLC analysis of plasma lipoprotein profile in *Fxr*$^{fl/fl}$ and *L-Fxr*$^{-/-}$ mice (n=8). (**B**–**F**) *Fxr*$^{fl/fl}$ and *L-Fxr*$^{-/-}$ mice were gavaged with either vehicle or OCA (n=8). After 7 days, mice were injected i.v. with J774 macrophages loaded with [^{3}H]cholesterol and RCT was performed as described in Methods. Plasma radioactivity (**B**), fecal [^{3}H]total sterols (**C**), fecal [^{3}H]free cholesterol (**D**), fecal [^{3}H]bile acids (**E**) and hepatic mRNA levels (**F**) were determined. * p<0.05, ** p<0.01. Unless otherwise indicated, the difference is shown when compared to vehicle-treated control mice.

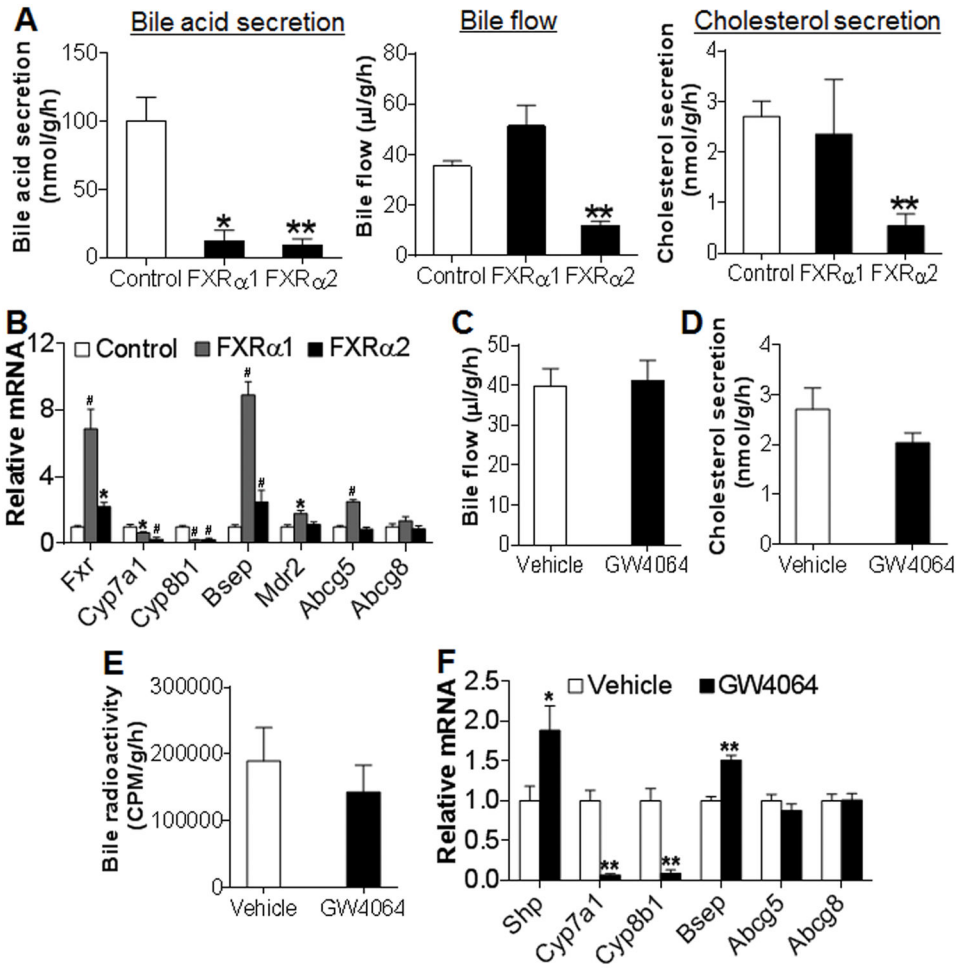

Figure 4. Activation of FXR does not increase biliary cholesterol secretion

(A, B) C57BL/6 mice were injected i.v. with Ad-VP16 (control), Ad-FXRα1-VP16 (FXRα1) or Ad-FXRα2-VP16 (FXRα2). After 7 days, gallbladder cannulation was performed. The rates of bile acid secretion (**A**, left panel), bile flow (**A**, middle panel) and biliary cholesterol secretion (**A**, right panel) as well as hepatic mRNA levels (**B**) were determined. (**C–F**) C57BL/6 mice were gavaged with either vehicle or GW4064. Bile flow rate (**C**) and biliary cholesterol secretion rate (**D**) were determined. In (**E**), C57BL/6 mice were also injected i.p. with J774 macrophages loaded with [^{3}H]cholesterol and bile [^{3}H]-radioactivity was determined after 48 h. In (**F**), hepatic mRNA levels were quantified. * p<0.05, **, # p<0.01. Unless otherwise indicated, the difference is shown when compared to the control mice or vehicle treatment group.

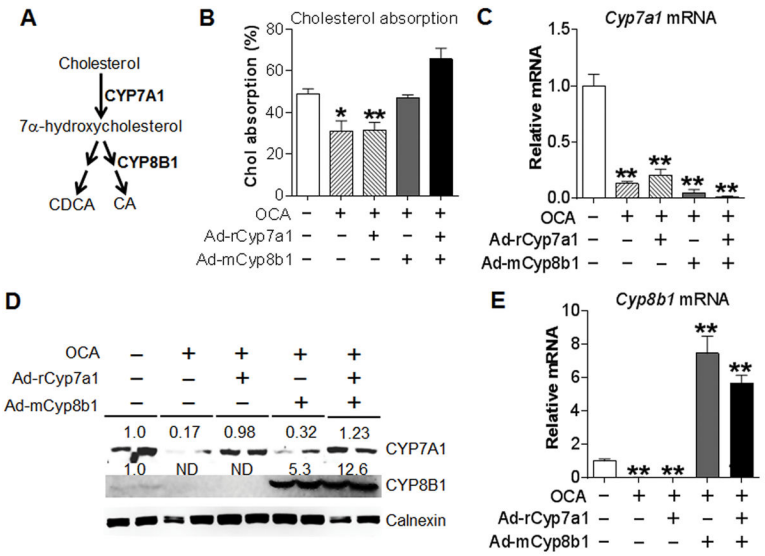

Figure 5. Re-expression of CYP8B1 alone or CYP7A1 plus CYP8B1 prevents OCA from inhibiting intestinal cholesterol absorption

(**A**) A diagram showing that CYP7A1 and CYP8B1 are key enzymes in the classic pathway of bile acid biosynthesis. (**B–E**) C57BL/6 mice were injected i.v. with a control virus, Ad-rCyp7a1 and/or Ad-mCyp8b1 on day 1. On day 2, mice were gavaged with either vehicle or OCA (n=6). On day 8, mice were given [^{3}H]cholesterol and [^{14}C]cholesterol and intestinal cholesterol absorption was performed using dual-isotope plasma ratio method (**B**). Hepatic *Cyp7a1* mRNA level (**C**), protein levels (**D**) and *Cyp8b1* mRNA level (**E**) were determined. * p<0.05, ** p<0.01. Unless otherwise indicated, the difference is shown when compared to the vehicle treatment group.

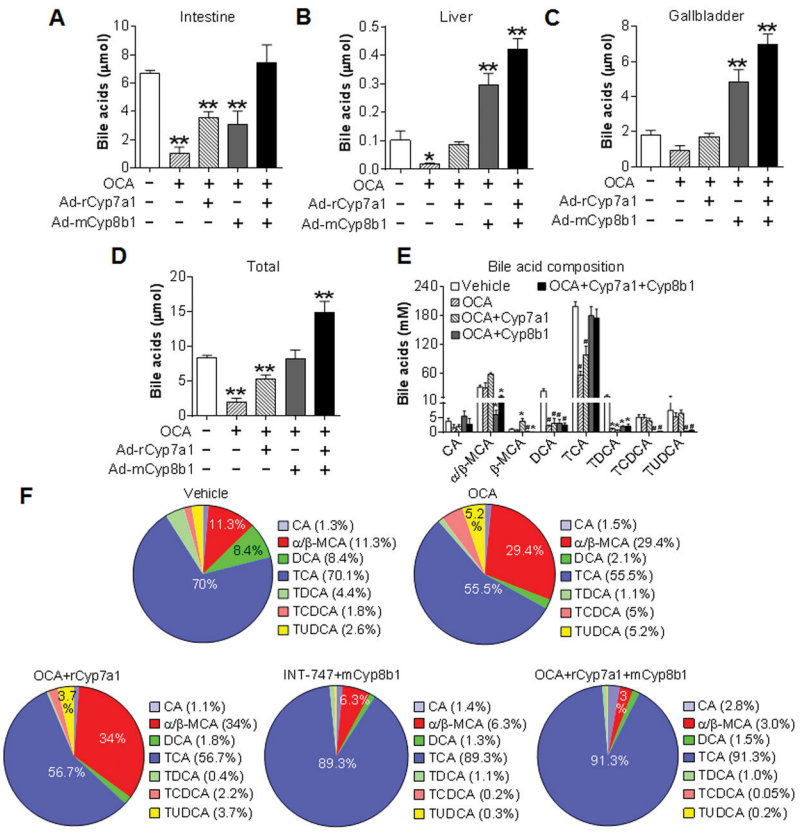

Figure 6. Re-expression of CYP8B1 alone or CYP7A1 plus CYP8B1 prevents OCA from altering TCA and MCA levels

(**A**–**F**) C57BL/6 mice were injected i.v. with a control virus, Ad-rCyp7a1 and/or Ad-mCyp8b1. One day later, mice were gavaged with either vehicle or OCA (n=6). Bile acid levels in the intestine (**A**), liver (**B**) and gallbladder (**C**) as well as the total bile acid levels (including intestine, liver and gallbladder) (**D**) were analyzed. Individual bile acid levels in the bile were quantified (**E**) and the composition (%) of individual bile acids under different treatments was shown (**F**). * $p<0.05$, ** $p<0.01$. Unless otherwise indicated, the difference is shown when compared to the vehicle treatment group.